ingegneria sismica
International Journal of Earthquake Engineering
Anno XLIII - Num. 3 - 2026

Triaxial test verification of LC yield surface evolution characteristics of unsaturated loess under different initial moisture contents

Jianxin Jing[1], *Shaoyan Wu*[1,*], *Yiping Jiang*[1] *and Zixuan Yin*[1]

[1] Geological Engineering and GeomaticsSchool of Chang'an University, Xi'an 710054, China

SUMMARY: *To investigate the influence of initial moisture content on the mechanical properties of unsaturated loess, this paper focuses on unsaturated loess with varying initial moisture content. Isotropic compression tests at constant moisture content and true triaxial shear tests were conducted. By controlling suction and net mean stress, the relationship between void ratio and net mean stress was analyzed to determine the yield point and yield stress. Furthermore, the effects of confining pressure, saturation, dry density, and clay content on yield characteristics were explored. The experimental results indicate that under isotropic compression at constant moisture content, the void ratio decreases with increasing net mean stress. The e-lnp curve is approximately composed of two intersecting straight lines, with the intersection point representing the isotropic compression yield stress. Both yield stress and yield suction increase with the increase of initial suction. The slopes of the straight lines before and after yielding are less affected by initial suction. Moisture weakens the structural yield characteristics of loess, and the yield stress of different soil samples exhibits varying trends with increasing saturation. The study reveals that initial moisture content significantly affects the LC yield characteristics of unsaturated loess. Yield stress is closely related to saturation, dry density, and clay content. The research findings provide a theoretical basis for the engineering application of unsaturated loess.*

KEYWORDS: *initial moisture content; unsaturated loess; LC yield surface; true triaxial shear test; yield stress; isotropic compression; saturation*

1 Introduction

Loess is a semi-arid sediment with certain regularity in geographical distribution and special engineering characteristics such as high natural porosity [1, 2]. In the process of sediment formation, certain minerals such as calcite can serve as binding materials, forming bridges between the original sediment particles and binding them together. Due to the low initial moisture content of loess sediments, the influence of suction on soil properties becomes very significant. Due to its complex properties, loess sediments have a stable structure in a naturally unsaturated state [3].

Unsaturated soil is also widely distributed, and it is easy to encounter unsaturated soil in engineering. The soil above the groundwater level is generally in an unsaturated state, and its saturation state generally changes continuously with the seasons and precipitation. Soil in dry or semi dry areas is often in an unsaturated state throughout the year [4]. The three-phase composition and characteristics of each phase component of unsaturated soil are different from those of saturated soil. Considering these factors, in addition to the net stress acting on the soil

*18732323277@163.com
https://doi.org/10.65102/is20261228
Published: 10 June, 2026

skeleton, unsaturated soil also has the effects of pore air pressure and pore water pressure. The matric suction of unsaturated loess has a significant impact on the physical properties of loess, and the model for this indicator can be defined and calculated by two indicators: water pressure and air pressure. The shrinkage film effect in unsaturated loess is mainly determined by the characteristics of the gas-phase medium, which determines that unsaturated loess has more complex mechanical properties than saturated loess [5]. Studying the strength and deformation characteristics of unsaturated loess is of great significance for the theoretical research and application of unsaturated loess.

Although the current theory of unsaturated soil mechanics has made significant progress, theoretical research is far less complete than that of saturated soil theory, and its application is much lagging behind, mainly due to the fact that unsaturated soil is much more complex than saturated soil [6]. Firstly, the pores of unsaturated soil contain both water and gas phases, and the water gas interface is formed by the contraction membrane tension between gas and liquid, as well as the adsorption force between solid and liquid, resulting in a saddle shaped meniscus [7]. This phenomenon can cause different air pressure and water pressure indicators in the pores of unsaturated loess materials, among which the water pressure indicator can be divided into two characteristics: negative pores and positive pores; Secondly, the presence of only water phase and gas water two-phase fluid in unsaturated loess material is different, which will result in more complex and variable deformation behavior of unsaturated soil; Finally, due to the gas occupying some of the pore channels in the soil, the discharge law of fluids in the pores is also relatively complex, and Darcy's law in saturated soil is no longer fully applicable to unsaturated soil [8]. In addition, unsaturated soil is not only subjected to self-weight stress and additional stress, but also to suction, which includes osmotic suction and matric suction.

Therefore, studying the suction and deformation strength characteristics of undisturbed loess under triaxial stress conditions with constant moisture content has important theoretical significance and practical value. This article takes unsaturated loess under different initial moisture content conditions as the research object, and conducts constant moisture content isotropic compression and triaxial shear tests on unsaturated loess with different initial suction. The suction, stress-strain, strength, and yield characteristics of unsaturated undisturbed loess under constant moisture content conditions are studied, and the changing characteristics and main influencing factors of the yield characteristics of unsaturated loess are explored.

2 Related Research

2.1 Study on Soil Water Characteristic Curve

The curve shape of the soil water characteristic curve is related to multiple factors such as the air intake value, residual moisture content, and dehumidification rate of the soil. The most important influencing factors of these soil water characteristic curves are the pore structure and mineral composition of the soil, while other factors affect the soil water characteristic curve through these two factors [9]. (1) The influence of internal factors. Due to the larger initial moisture content of the soil sample, the larger the diameter of its internal pores. Therefore, when the matric suction is low, water will be expelled from the soil, and the soil's air intake value will decrease with the increase of the initial moisture content of the soil. Scholars have found through experiments that there is a significant difference in the soil water characteristic curves between undisturbed soil and remolded soil. Undisturbed soil has a lower air intake value, a slower dehydration rate, and better water holding performance compared to remolded soil. This is mainly because in the long-term formation process of undisturbed soil, the soil particles have a certain directionality, and the pore structure formed contains interconnected drainage channels.

When dehumidified, gas is relatively easy to enter the pores, resulting in a lower intake value; The pore structure of reshaped soil lacks directionality, making it difficult for gas to enter, ultimately resulting in a higher intake value [10]. (2) External influencing factors. The stress history of soil is an important external factor that affects the soil water characteristic curve. As the pre compression consolidation stress increases, the sample becomes denser and the pore size is relatively smaller, making it difficult for gas to enter the soil. Therefore, the higher the pre compression consolidation pressure of the soil, the greater its inlet value, but the slower its dehydration rate. The confining pressure of soil is also an important external influencing factor. The hysteresis phenomenon of the soil water characteristic curve is particularly evident when the confining pressure is zero, and the higher the confining pressure, the greater the intake value and residual value [11]. In addition, the influence of factors such as fine particle content, compressibility, wet dry history, temperature, and multi factor coupling on the soil water characteristic curve cannot be completely ignored. (3) Current status of research on influencing factors. Many scholars have long noticed the influencing factors of unsaturated soil water characteristic curves and conducted research on them. Bahloul et al. [12] compared and analyzed the soil water characteristic curves of four different types of soil, and found that the soil's air intake value, residual volumetric water content, and water holding capacity all increased with the increase of clay content in the soil. Yates et al. [13] selected two types of unsaturated loess with different initial dry densities, and analyzed the influence of stress state on soil water characteristic curve under no pressure, uniform pressure, bias pressure, as well as loading and unloading stress conditions. Francisca et al. [14] analyzed the influence of clay content in soil on the soil water characteristic curve, and pointed out that when the suction is the same, the volumetric water content of soil increases with the increase of clay content. Fraters et al. [15] conducted experiments on debris containing different mineral compositions and studied the effects of factors such as fine particle content, average particle size, and porosity on the soil water characteristic curve. The study showed that the initial moisture content of the sample has a significant impact on its structural properties. In addition, many scholars have studied the coupling effect of multiple factors on the soil water characteristic curve, and have obtained many valuable conclusions.

2.2 Study on Strength Characteristics of Unsaturated Soil

For unsaturated soil, it has a three-phase medium, and the neutral stress in the unsaturated effective stress principle is composed of an equivalent pore stress composed of pore water pressure and pore gas pressure [16]. Therefore, its mechanical shape is much more complex than that of saturated soil. Usually, unsaturated soil exhibits obvious shrinkage film characteristics between the gas and liquid phases. The change of shrinkage film can affect the characteristics of unsaturated soil, and its existence can contribute to the strength of the soil and reduce the permeability coefficient. Matrix suction is also a representative parameter when studying unsaturated soil. For structural loess, the influence of changes in moisture content on structural connections and matric suction cannot be ignored. In unsaturated soil, matric suction increases with the decrease of moisture content, and the changes are nonlinear, making it difficult to accurately grasp the strength characteristics of unsaturated soil [17].

According to existing research, matric suction has a strengthening effect on soil, and also has a significant impact on the shear strength index, cohesion, of soil. Most experimental results show that within the suction range studied in the experiment, the influence of matric suction on the internal friction angle is not significant, while the cohesive force varies significantly with suction, and the cohesive force of unsaturated soil is always greater than that of saturated soil. Vahdani et al. [18] found through experimental research that matric suction has a significant

effect on the cohesion and internal friction angle of unsaturated silty clay, sandy silt, and fine sand. The variation of matric suction in unsaturated soil can affect soil strength, which has become a consensus. However, it is currently unclear how suction specifically affects the strength of unsaturated soil, that is, to what extent the variation of suction affects the strength parameters of unsaturated soil. Therefore, it is necessary to study the strength characteristics of unsaturated undisturbed soil from the perspective of soil structure [19].

Through true triaxial shear tests of unsaturated remolded loess under equal *b* conditions with 4 consolidation confining pressures, 5 medium principal stress ratios, and 2 matric suction, it was found that the shear stress increased with the increase of confining pressure, and the larger the confining pressure, the smaller it became; The greater the matric suction, the greater the shear stress, revealing the various mechanical properties of unsaturated soil under complex triaxial stress conditions. So far, there is still very little research on the strength and deformation characteristics of unsaturated loess under true triaxial conditions, so it is meaningful to combine the middle principal stress parameter b with matric suction to study the strength and deformation problems of unsaturated soil [20].

2.3 Study on Yield Characteristics of Unsaturated Loess

The yield characteristics of unsaturated soil are an important part of the constitutive relationship research of unsaturated soil. Among the proposed elastic-plastic stress-strain relationships of unsaturated soil, the most typical one is the constitutive model proposed by Alonso: there are two yield curves in the p-s plane, namely the suction increasing yield curve (SI curve) and the load collapsing yield curve (LC curve), where the SI yield curve is a straight line that increases suction to yield the soil, and the LC yield curve is a curve that increases load or decreases suction to yield the soil. The area enclosed by these two yield lines is what we call the elastic zone. When any stress path exceeds these two yield lines, the soil will yield. Meye et al. [21] conducted multiple experiments to control suction and net average stress, which not only verified the LC yield line on the p-s plane, but also improved the yield conditions of the original SI yield line.

(1) Isotropic compression yield characteristics. 1) Isotropic loading yields. The yield point of soil can be determined by conducting isotropic compression tests under controlled suction conditions. The obtained yield point can be plotted on the p-s plane and connected into a curve to obtain an LC curve. In the stress point area to the left of the curve, increasing the net average stress or decreasing suction (wetting) will reach the curve and yield [22]. The relationship between porosity and matric suction under isotropic compression net stress conditions in unsaturated soil can be determined by the *e*-log*p* curve. The stress points below the curve will yield when the suction increases and reaches the SI curve. Therefore, when describing the yield characteristics of unsaturated soil, two yield lines on the p-s plane, namely LC and SI curves, can be used to describe it. The greater the suction force, the greater the isotropic compressive yield stress. However, both tests for determining the LC yield line and the SI yield line are based on controlling one stress state variable (suction or net average stress), while the other stress state variable is changing separately. In reality, both stress states are changing, so the two yield lines are interrelated. Therefore, the two yield lines should be studied together.

(2) Shear yield characteristics of unsaturated soil. Unsaturated soil not only yields under equal compression conditions, but also yields under shear conditions. When using the *e*-log*p* curve under equal compression conditions to determine the yield point, it is considered that shear shrinkage strain will also occur during the shearing process, resulting in a relatively discrete yield point on the *p*-*q* plane. Fang Pham et al. [23] conducted triaxial equi beta shear tests on unsaturated remolded loess. As the yield of the soil during the shear process mainly depends on the influence of the deviatoric stress *q*, he used the V-9 relationship curve to

determine the yield point of the soil. Mohsen & Albusoda [24] defines the yield stress of unsaturated remolded loess at the boundary point (*p*, *q*) between the two stages of the E-log (*q*/*p*) relationship curve, and plots the yield stress point in the *p*-*q* plane; Bakhtiyar & Barno [25] approximated the beginning and end of the *e*-log (*q*/*p*) curve with straight lines, and used the stress values corresponding to the intersection of the two lines as the yield stress (p_y, q_y). They then plotted the (p_y, q_y) values of each experimental point on the *p*-*q* plane; The distribution of yield points obtained has good regularity, and the yield curve will expand outward with the increase of suction. The net yield stress and yield deviatoric stress obtained will increase with suction. At the same suction or moisture content, the yield deviatoric stress and the average yield net stress show a linear relationship.

3 Related Models

3.1 The Influence of Humidity Status on Strength Parameters

The shear strength of loess is mainly controlled by its moisture content. As the moisture content increases, the shear strength gradually decreases, manifested as a decrease in cohesion *c* and internal friction angle φ. The usual practice is to measure the main stress σ_1 under at least three different triaxial stresses σ_3, and then make at least three Mohr circles with $\left((\sigma_1+\sigma_3)/2,0\right)$ as the center and $(\sigma_1-\sigma_3)/2$ as the radius in the σ-τ coordinate system. Using the method of making three circles' common tangent lines (oblique line 1 in Figure 1), the values of *c* and φ are obtained [26].

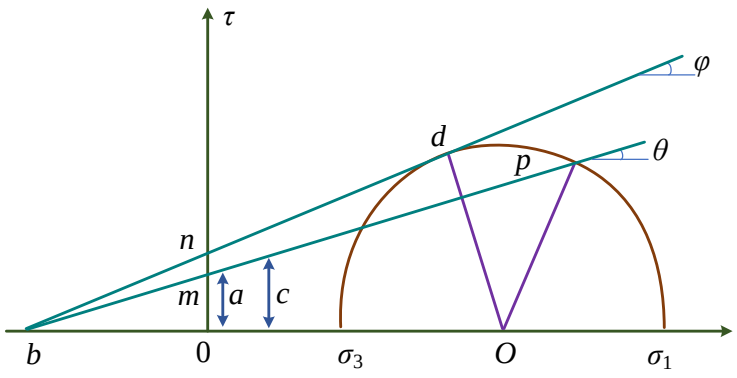

Figure 1: Schematic diagram of strength parameter calculation

Due to the fact that the common tangent line is simplified from a curved strength envelope, the straight-line type common tangent line can hardly be tangent to three Mohr circles at the same time, resulting in a certain degree of arbitrariness in the strength parameters used for graphical calculation. The author uses the relationship between line 2 and line 1 in Figure 1 to calculate the strength parameters *c* and φ values. Firstly, the maximum shear stress points (vertices) $\tau_{\max}=(\sigma_1-\alpha_3)/2$ of each Mohr circle are identified from the experimental data. Then, these maximum shear stress points are linearly fitted to obtain line 2, which is [27]:

$$\begin{cases} c = a/\cos\varphi \\ \sin\varphi = \tan\theta \end{cases} \tag{1}$$

where, a and θ are the intercepts and inclinations of Line 2; c, φ is the intercept and dip angle of the intensity envelope line 1.

3.2 Validation of Yield Criteria

Research has shown that the conditions for plastic yield of loess satisfy the Mohr Coulomb shear yield condition. However, due to the irregular hexagonal curve projected onto the element plane, the handling of the sharp points, edges, breakpoints, and lines of the hexagon during numerical analysis can cause many unexpected troubles [28]. Moreover, it can lead to complex calculations and slow convergence. Therefore, seeking a continuous and smooth convex curve projected onto the plane is very meaningful for numerical analysis of loess. In recent years, the D-P yield condition has been widely used in the plastic analysis of geotechnical materials. It is a special case of the generalized von Mises yield condition, and its projection on the π plane satisfies the conditions of continuity and smoothness. The author verified the applicability of the D-P yield criterion in the plastic yield of loess by analyzing the results of conventional triaxial tests on loess with different moisture contents. The yield criterion for D-P is [29]:

$$\alpha I_1 + \sqrt{J_2} = K \tag{2}$$

where,

$$\begin{cases} \alpha = \dfrac{\tan\varphi}{\sqrt{9+12\tan^2\varphi}} \\ I_1 = 3\sigma_m \\ K = \dfrac{3c}{\sqrt{9+12\tan^2\varphi}} \\ J_2 = \dfrac{1}{6}\left[(\sigma_1-\sigma_2)^2+(\sigma_2-\sigma_3)+(\sigma_3-\sigma_1)^2\right] \end{cases}$$

After processing the experimental data according to equation (2), it was placed in the $\sqrt{J_2}$-I_1 coordinate system (Figure 2). The results show that the yield equation of loess under different moisture contents is approximately a straight line, indicating that the yield conditions of loess also comply with the D-P criterion. This greatly facilitates the numerical analysis of the elastic-plastic properties of loess.

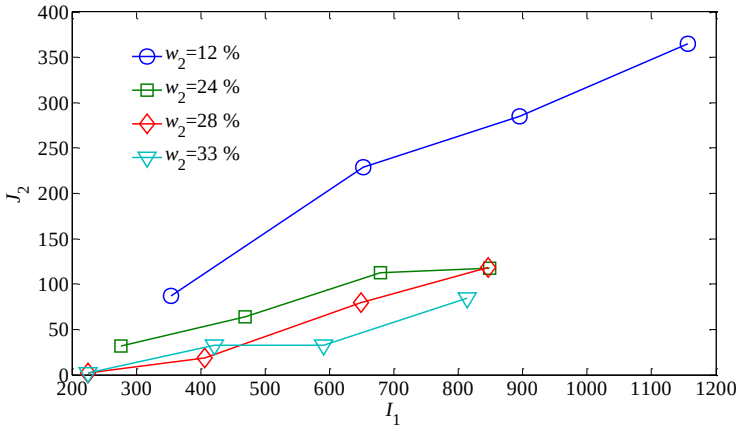

Figure 2: D-P yield criterion

4 Experimental Setup

4.1 Test Soil Sample and Test Plan

The experimental soil is Q3 undisturbed loess taken from a certain region in China, with physical properties including specific gravity G=2.70, moisture content w_0=15.58%, porosity e_0=0.967, liquid limit w_L=31.19%, and plastic limit w_p=19.75%. Cut a sample with a diameter of 3.87cm and a height of 8cm. To reduce the impact of differences in dry density, samples with a dry density difference of less than 0.02g/cm^3 were selected.

In order to study the deformation strength characteristics of undisturbed loess with different humidity levels, samples with a natural moisture content of w0 were controlled by increasing or decreasing the moisture content. When $w<w_0$, the air-drying method was used, and when $w>w_0$, the titration water injection method was used. After air drying or adding water to reach the controlled moisture content, the samples were placed in a sealed container for more than 72 hours to ensure uniform moisture diffusion. The sample was saturated using the suction saturation method, and the final saturation reached over 95%. The controlled net confining pressure is 100, 200, 300, 400 kPa. The experimental equipment and instruments used are shown in Figure 3.

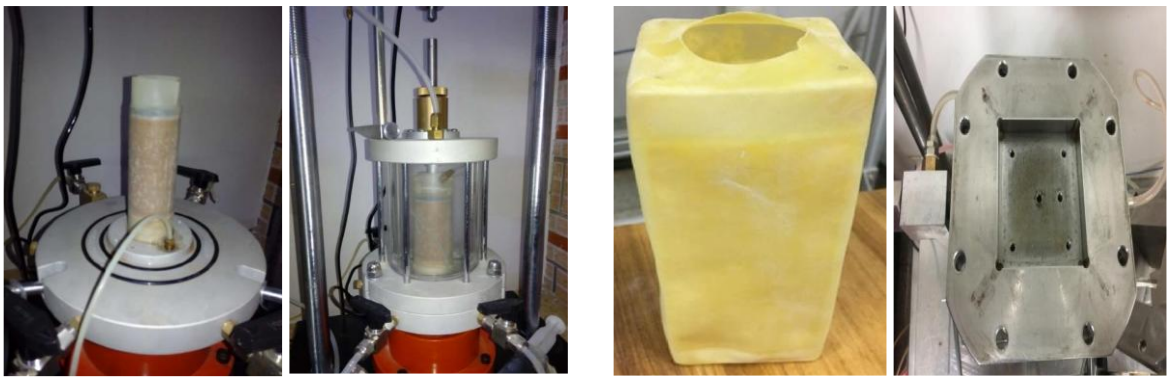

(a) Pressure chamber (b) Rubber bag and base

Figure 3: Experimental Equipment

4.2 Test Soil Sample and Test Plan

The true triaxial apparatus developed by a research institute in China is characterized by the use of a one chamber four chamber mechanism with vertical rigidity and lateral flexibility loading, as well as a servo stepper motor-driven hydraulic cylinder, to apply principal stresses of different sizes in three directions and measure principal strains in three directions. Compared with conventional triaxial apparatus, this instrument can truly simulate the principal stress state of soil. Moreover, it can automatically control different stress paths and test the mechanical properties of the king. This article focuses on the requirements of unsaturated soil testing under true triaxial stress conditions. Ceramic plates and permeable plates are installed on the base of the pressure chamber and the top cover of the specimen of the true triaxial apparatus, respectively. Control and measurement devices for pore gas pressure and pore water pressure are added, and axial translation technology can be used to control and measure matrix suction for true triaxial compression testing. This article selects samples with a dry density difference of less than 0.01g/cm and a natural moisture content difference of less than 1%, cuts and prepares them into rectangular specimens, and then prepares the specimens into different moisture contents through humidification or dehumidification. For samples with a moisture

content lower than natural, the method of natural air drying is used; The sample with higher natural moisture content shall be sprayed with spray water. After the sample reaches the required moisture content for preparation, it should be placed in a sealed moisturizing cylinder for at least 96 hours (the time for uniform moisture transfer is determined through comparative testing during the preparation stage) to ensure even diffusion of moisture.

The unsaturated loess test includes true triaxial net stress isotropic consolidation compression test and true triaxial net stress compression shear test with different values of principal stress b. During the experiment, first place the sample bottom plate embedded in the clay plate (saturated) into a specially made latex film, and use screws to pass through the bottom plate screw holes, latex film holes, and sealing gaskets, tightly connecting and fixing it to the pressure chamber base. And ensure that the drainage holes on the bottom plate of the sample are sealed and connected to the drainage holes on the pressure chamber base. It is worth noting that when installing the sample, it is necessary to ensure the sealing between the latex film at the bottom of the sample, the permeable bottom plate, and the pressure chamber. Otherwise, air and water leakage may occur, making it difficult to control the moisture content or suction of the sample. Then, install the split sample mold on the pressure chamber base, with its bottom end embedded in the groove of the pressure chamber base, and seal it with Vaseline. The latex film is flipped outward at the top of the sample mold, wrapped around the top, and tightly adhered to the inner wall of the sample mold. If the latex film is not tightly attached to the inner wall of the sample mold, the method of vacuuming can be used to suck the air between the two, which can promote the latex film to adhere to the inner side of the sample mold. Carefully place the undisturbed sample inside the latex film to avoid friction between the sample and the latex film, which can damage the edges and corners of the sample. You can also apply a layer of talcum powder on the inside of the latex film to reduce friction. After the bottom of the sample is completely placed on the clay plate, turn off the vacuum suction device, place a dry filter paper on the top of the sample, place the porous plate, flip the latex film, and the latex film just wraps around the upper porous plate.

Place special sealing gaskets and sample caps on the porous plate in sequence, thread screws through the four screw holes of the sample cap, sealing gaskets, latex film, and upper porous plate, tighten the screws to form a sealed whole, and thus complete the sealing of the sample. Next, install the pressure chamber with its side wall fixed to the base. The four walls of the pressure chamber are separated into four chambers by isolation plates, which can accommodate hydraulic bags on the side of the sample. Reinstall the pressure chamber cover and fix it on the side wall of the pressure chamber. Connect the axial force transmission rod and vertical displacement sensor, and the sample installation is completed. The pressure chamber base is equipped with inlet and outlet holes, with a water stop valve connected to the inlet hole and a high-precision pore pressure sensor connected to the outlet hole through a three-way valve. By closing the two valves, the pore water pressure can be measured through the pore pressure sensor, and stable pore air pressure can be applied to obtain matrix suction. The standard for stable sample suction is that the suction change is less than 0.5kPa/h. After the initial suction of the sample stabilizes, during the isotropic compression consolidation process, the standard for determining the stability of suction after multiple tests is 20, 24, and 30 hours. The change in suction at 24 and 30 hours is less than 0.5 kPa/h. Therefore, it is considered that the suction of the sample has reached stability after 20 hours. Therefore, in this study, the consolidation time of unsaturated soil is set to 24 hours. Air pressure and consolidation confining pressure are applied to enter the consolidation stage, and the consolidation deformation and matric suction are measured. After consolidation is completed and the suction reaches stability, a shear test with a constant value of the main stress parameter b is conducted, with a set shear rate of 0.005mm/min. The experiment adopts strain control, and the end condition of the experiment

is set to axial strain reaching 12%, that is, deformation reaching 16.8mm, which is considered as sample failure. After the suction stabilizes, the experiment ends. The shearing process conforms to the experimental conditions of unsaturated aqua regia, slow gas-phase movement, and small abrupt changes, which is reasonable. Throughout the entire experiment, the drain valve on the instrument base was closed, the air pressure remained constant, and the pore water pressure constantly changed.

5 Result Analysis

5.1 Yield Characteristics

The initial suction s_0 (the average value at the same moisture content), initial saturation Sr0, and isotropic compression saturation S_{rc} of the sample are shown in Table 1.

Table 1: State characteristics of specimens in triaxial tests with constant moisture content

σ_3/kPa	initial			After isotropic compression		During shear failure		
	w/%	s0/kPa	Sr0/%	sc/kPa	Src/%	sf/kPa	Srf/%	β/%
100	13.0	378	35.8	369	37.0	357	40.3	-0.3
200	13.0	378	35.8	369	37.2	357	42.7	3.0
300	13.0	378	35.8	334	37.5	346	45.6	3.5
400	13.0	378	35.8	332	37.9	341	47.3	3.1
100	15.6	176	40.9	175	42.2	189	49.2	8.8
200	15.6	176	40.9	171	43.0	189	55.5	10.9
300	15.6	176	40.9	154	44.0	181	57.1	16.6
400	15.6	176	40.9	143	45.3	180	62.8	25.2
100	18.0	85	45.6	85	47.2	108	61.9	27.8
200	18.0	85	45.6	81	48.5	119	64.7	46.0
300	18.0	85	45.6	81	50.1	105	69.5	31.6
400	18.0	85	45.6	76	51.4	113	75.4	47.8
100	20.5	39	50.3	37	52.2	64	75.0	71.7
200	20.5	39	50.3	35	54.3	60	80.2	65.3
300	20.5	39	50.3	34	58.8	67	93.0	89.8
400	20.5	39	50.3	32	64.3	64	99.5	90.7

Prepare samples with different moisture contents (including 13.0%, 15.6%, 18.0%, 20.5%, 36.0% (saturated moisture content)) by increasing or decreasing the humidity. When the maximum level net average stress $p(p=\sigma_3)$ is 400 kPa, the *e*-ln*p* relationship between porosity e and net average stress p is shown in Figure 4.

From Table 1 and Figure 4, it can be seen that:

(1) Under the action of isotropic compressive stress with constant moisture content, the compression and discharge of pore gas reduce the volume of unsaturated loess samples, and the porosity e decreases with the increase of net average stress *p*. *e*-ln*p* is approximately located on the intersection of two straight lines, and the net average stress at the intersection is the isotropic compressive yield stress p_{y0}. The suction force s_{y0} values for p_{y0} and yield point are determined in Table 2. It can be seen that both p_{y0} and s_{y0} increase with the increase of s_0, $s_0=380\text{kPa}$; When $p=400\text{kPa}$ (due to instrument limitations, only a total confining pressure of 800kPa can be applied), the *e*-ln*p* curve has not yet shown a turning point, that is, it has not yielded. These are mainly due to the structural increase of unsaturated loess with the increase of initial suction.

(2) The slope k_0 of the e-lnp line before and after yielding is shown in Table 2. It can be seen that k_0 slightly decreases with the increase of s_0, and the influence of initial suction can be ignored. Its average value is approximately 0.03; λ_0 increases with the increase of s_0, and changes significantly when s_0 is small ($s_0 \leq 41$kPa), while changes are small when s_0 is large (s_0 >41kPa).

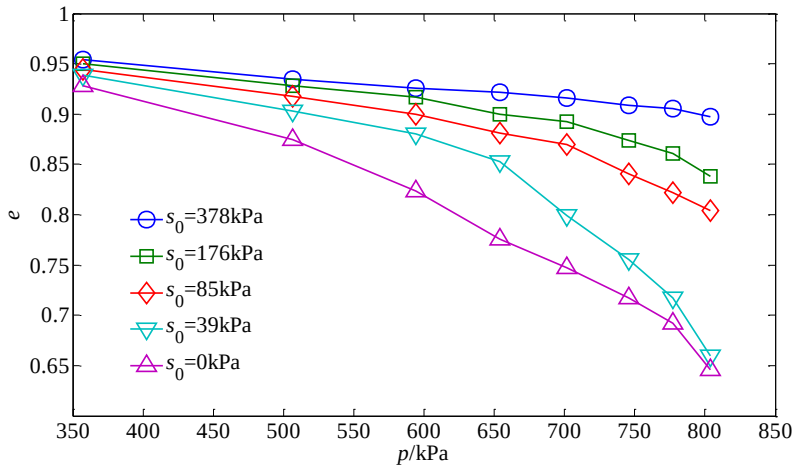

Figure 4: e-lnp curve of isotropic compression test with constant moisture content

Table 2: Soil parameters of triaxial test with constant moisture content

w/%	s_0/kPa	p_{y0}/kPa	s_{y0}/kPa	k_0	λ_0	*h*/kPa	*c*/kPa	*M*	λ
13.0	378	>400	<329	0.015	—	237	113	0.908	0.149
15.6	176	360	134	0.027	0.235	192	90	0.908	0.149
18.0	85	310	78	0.035	0.216	125	55	0.908	0.149
20.5	40	210	32	0.038	0.214	91	48	0.908	0.149
36.0(saturated)	0	110	0	0.042	0.121	49	18	0.908	0.103

5.2 Factors Affecting Yield Characteristics

The soil samples used in the experiment were collected from four typical loess slopes in China, with a depth of 4-5m, all of which were Malan loess of the Upper Pleistocene (Q) aeolian origin. The soil sample is light gray yellow in color, with uniform texture and loose structure, and visible large pores with the naked eye. Its basic physical properties show that all four groups of loess samples are medium plasticity clayey silt. From Table 3, it can be seen that there are significant differences in the dry density and porosity of the Malan loess used in the experiment, as well as some differences in the particle content. For simplicity, the four sets of samples are labeled as XGA, XJB, TSC, and WCD.

As mentioned earlier, the structural yield characteristics of shallow unsaturated loess are closely related to confining pressure, saturation (water content), and physical properties. Dry density and clay content are the main physical properties that control the stability of loess structural systems. Therefore, based on the statistical relationship between confining pressure, saturation, dry density, clay content, and structural yield stress, this article explores the changing characteristics of yield characteristics of unsaturated loess. Due to the fact that the saturation levels of each sample were not completely consistent during the experiment, only the test results at saturation levels of 20% and 50% were presented in the analysis of the impact on dry density and clay content.

Table 3: Basic Physical Properties of Loess Samples

Test Name	Excavation depth (m)	Dry density (kN/m^3)	void ratio	Liquid limit (%)	Plastic limit (%)	Particle size (mm) and its content (%)		
						clay particle 0.005	powder particles 0.005~0.075	sand > 0.075
XGA	4.19	14.67	0.85	27.32	11.75	18.01	78.74	3
XJB	4.08	16.28	0.70	29.39	18.48	34.27	62.56	3
TSC	4.03	14.17	0.91	28.01	18.03	26.36	70.36	3
WCD	4.38	12.56	1.18	26.87	16.32	16.51	79.84	4

Similar to previous research based on compression tests, moisture significantly weakened the yield characteristics of loess structures (Figure 5). However, the influence trend of saturation on the structural yield stress of each group of soil samples is not completely consistent. The structural yield stress of XJB, XGA, and TSC soil samples shows a clear quadratic nonlinear decreasing trend with increasing saturation. The structural yield stress decreases by more than 80% at 90% saturation compared to 20% saturation; The structural yield stress of WCD specimens has a good linear relationship with saturation, and the structural yield stress decreases by about 50% at a saturation of 60% compared to 20%.

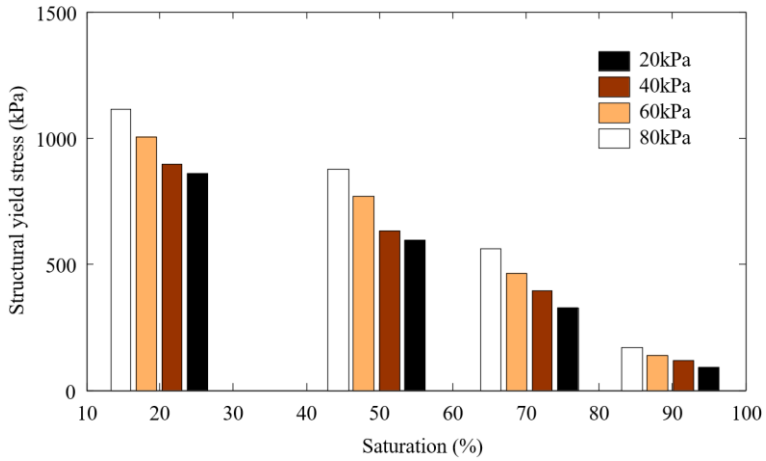

(a)XJB

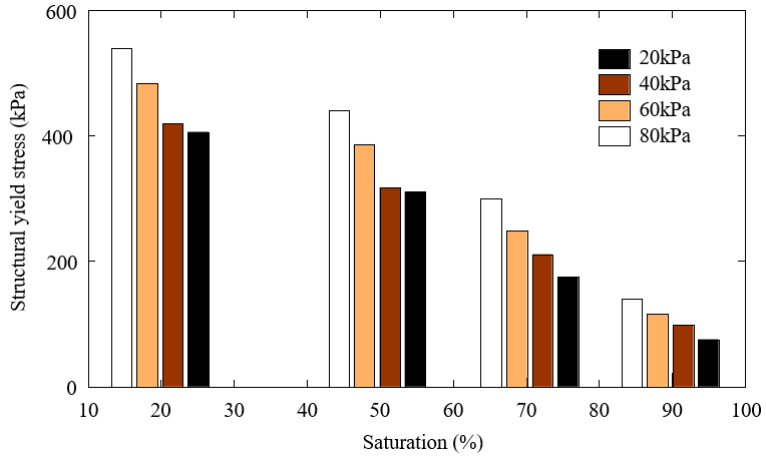

(b)XGA

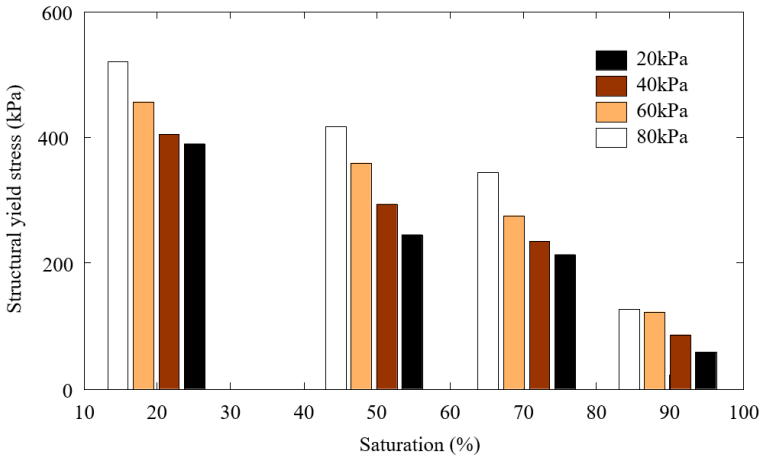

(c)TSC

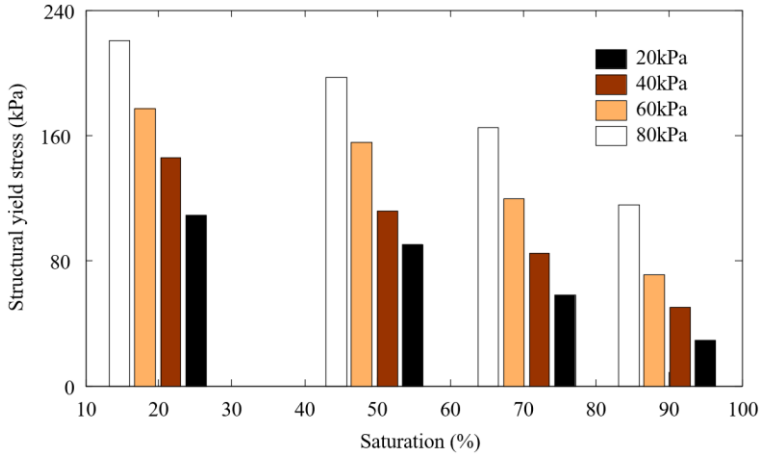

(d)WCD

Figure 5: Relationship curve between structural yield stress and saturation

The relationship between structural yield stress and saturation is closely related to the unique structure of loess. Due to its unique growth environment, loess has formed an elevated structural system with coarse silt as the skeleton and clay particles and salt as the binder. When the saturation is low, not only is there strong bonding between clay particles and salt in the soil, but also strong matric suction (capillary force) is recommended in the intergranular pores, resulting in a higher structural yield stress of the royal body. When the moisture content in the soil increases, not only does the water film on the surface of the clay particles thicken, soluble salts gradually dissolve, and the bonding effect between particles weakens, but the matric suction between particles also gradually decreases, resulting in a decrease in structural yield stress. So the inherent mechanism of loess instability when the saturation is high is its lower structural yield stress.

6 Conclusion

This article systematically studied the LC yield surface evolution characteristics of unsaturated loess under different initial moisture content conditions through isotropic compression and true triaxial shear tests. The main work includes conducting isotropic compression and shear tests

on unsaturated loess samples with different initial suction forces. By controlling the suction force and net average stress, the relationship between porosity and net average stress is analyzed in depth, and the determination method of yield point and yield stress is clarified. The specific conclusion is as follows:

(1) Under the condition of triaxial shear stress with constant moisture content, as the deviatoric stress and saturation increase, the suction force first decreases or remains basically unchanged before increasing; When the initial suction force is the same, the net confining pressure has little effect on the suction force during shear failure; When shear failure occurs, the suction force increases with the increase of initial suction force, and the rate of change of suction force decreases significantly with the increase of initial suction force.

(2) Under the condition of constant water content and isotropic compressive stress, the compressibility index changes significantly at low suction, while it changes less at high suction (s_0>41kPa); The suction decreases with the increase of net average stress and saturation, and the initial suction has little effect on the rate of suction change.

(3) The isotropic compressive yield stress, shear yield net average stress, and yield deviatoric stress all increase with the increase of initial suction; During the triaxial shear process with constant moisture content, the e-ln$p$ curve before yielding slowly decreases along a straight line with the same slope as the isotropic compression line before yielding or before yielding, and rapidly decreases after yielding.

Although this article has achieved certain results in the study of the evolution characteristics of LC yield surface in unsaturated loess, there are still many unknown areas that need further exploration. Future research can further consider the effects of temperature changes, loading rates, and multi field coupling on the yield characteristics of unsaturated loess. In addition, combining numerical simulations and practical engineering cases to deeply explore the mechanical behavior of unsaturated loess in different engineering environments is also an important direction to enhance the theoretical research and application value. Through these studies, we are expected to have a more comprehensive understanding of the mechanical properties of unsaturated loess, providing more scientific and reasonable guidance for related engineering design and construction.

Funding

The research described in this paper was financially supported by the Natural Science Foundation of Shaanxi Province (Grant Nos. 2023-LL-QY-42 and 2025JC-YBMS-274), and the Fundamental Research Funds for the Central Universities, CHD (Grant No. 300102265202).

About the Author

Jianxin Jing was born in Zhang jiakou, He bei. China, in 2000. He will obtained a master's degree from Chang’an University in China 2026. He currently studying at the School of Geological Engineering and Geomatics, Chang’an University. His main research direction is Geological Engineering.

Shaoyan Wu was born in Yantai, Shan dong. China, in 1985. She obtained a Doctorate degree from China University of Geosciences, Beijing in China 2015. She currently teaching at the School of Geological Engineering and Geomatics, Chang’an University. Her main research direction is Geological Engineering.

Yiping Jiang was born in Mianyang, Si chuan. China, in 1999. She obtained a master's degree from Chang’an University in China. She currently studying at the School of Geological

Engineering and Geomatics, Chang'an University. Her main research direction is Geological Engineering.

Yi-ping JIANGwas born in Hai kou, Hai nan. China, in 2000. He will obtained a master's degree from Chang'an University in China 2026. He currently studying at the School of Geological Engineering and Geomatics, Chang'an University. His main research direction is Geological Engineering.

References

[1] Yates K, Russell A R. The unsaturated characteristics of natural loess in slopes, New Zealand[J]. Géotechnique, 2023, 73(10): 871-884.

[2] Yates K, Russell A. The hydromechanical behaviour of unsaturated loess in slopes, New Zealand[C]//E3S Web of Conferences. EDP Sciences, 2023, 382: 24007.

[3] McDowell T M, Mason J A, Vo T, et al. Hydrology of a Semiarid Loess-Paleosol Sequence, and Implications for Buried Soil Connection to the Modern Climate, Plant-Available Moisture, and Loess Tableland Persistence[J]. Journal of Geophysical Research: Earth Surface, 2022, 127(12): e2022JF006800.

[4] Hamed S, Ali K, Mohammad-Mehdi A. Slope stability of an unsaturated embankment with and without natural pore water salinity subjected to rainfall infiltration[J]. Rock and Soil Mechanics, 2022, 43(8): 5.

[5] Yates K, Russell A R. Field measurements and modelling of climate-driven hydraulic flux, water content, and suction in a loess slope[J]. Canadian Geotechnical Journal, 2024, 62: 1-19.

[6] Al-Obaidi Q A, Schanz T. Deformation of unsaturated collapsible soils under suction control[J]. Journal of the Mechanical Behavior of Materials, 2022, 31(1): 623-630.

[7] Giomi I, Francisca F M. Experimental and Numerical Analysis of the Behavior of Collapsible Loess under Infiltration of Nonaqueous Phase Liquids[J]. Journal of Hazardous, Toxic, and Radioactive Waste, 2024, 28(2): 04024002.

[8] Al-Obaidi Q A, Schanz T. Soil–water characteristic curve of unsaturated collapsible soils[J]. Journal of the Mechanical Behavior of Materials, 2023, 32(1): 20220210.

[9] Giomi I, Francisca F M. Numerical modeling of the oedometrical behavior of collapsible loess[J]. Geotechnical and Geological Engineering, 2022, 40(5): 2501-2512.

[10] Gramegna L, Abed A A, Sołowski W T, et al. A constitutive framework for the chemo-mechanical behaviour of unsaturated non-expansive clays[C]//E3S Web of Conferences. EDP Sciences, 2023, 382: 15004.

[11] Tankiewicz M, Kowalska M, Mońka J. Evaluation of Shear Strength and Stiffness of a Loess–Sand Mixture in Triaxial and Unconfined Compression Tests[J]. Materials, 2024, 17(15): 3831.

[12] Bahloul O, Tebbi F Z, Lekouara L. Experimental study of the physico-chemical stabilization of a loess by sodium silicate: Case of southern Algeria[J]. Selected Scientific Papers-Journal of Civil Engineering, 2023, 18(1): 20230013.

[13] Yates K, Chiaro G, Pokhrel A, et al. Liquefaction potential of reconstituted New Zealand loess[J]. Japanese Geotechnical Society Special Publication, 2024, 10(12): 323-328.

[14] Francisca F M, Giomi I, Rocca R J. Inverse analysis of shallow foundation settlements on collapsible loess: Understanding the impact of varied soil mechanical properties during wetting[J]. Computers and Geotechnics, 2024, 167: 106090.

[15] Fraters D, Ros G H, Brussée T. Measuring Nitrate Leaching in the Vadose Zone of Loess Soils—Comparison of Batch Extraction and Centrifugation[J]. Water, 2023, 15(15): 2709.

[16] Pineda J, Dinh H L. Evolution of K0 in compacted loess upon loading and wetting paths[C]//E3S Web of Conferences. EDP Sciences, 2025, 642: 03020.

[17] Tankiewicz M, Kowalska M. Stiffness moduli in triaxial tests on a loess-sand mixture[C]//E3S Web of Conferences. EDP Sciences, 2024, 544: 11011.

[18] Vahdani M, Hajitaheriha M M, Hasani Motlagh A, et al. A modified two-surface plasticity model for saturated and unsaturated soils[J]. Indian Geotechnical Journal, 2022, 52(4): 865-876.

[19] Nepelski K. Geotechnical interpretation of the geological structure of loess covers in Lublin Region[J]. Architecture Civil Engineering Environment, 2023, 16: 101-110.

[20] Vojtíšek J, Bruthans J. Loess susceptibility to erosion: Interaction of cohesion sources, air slaking and confinement[J]. Earth Surface Processes and Landforms, 2024, 49(6): 1821-1835.

[21] Meye S M, Nguema P F, Fomeza M P T, et al. Seepage Control of Irrigation Water: A Critical Constituent in Disaster Avoidance and Loess Project Management[J]. International Journal of Water Management and Diplomacy, 2022, 1(8): 79-93.

[22] Haeri S M, Soleymani Borujerdi S, Akbari Garakani A. Effects of initial shear stress on the hydromechanical behavior of collapsible soils[J]. Acta Geotechnica, 2023, 18(11): 6051-6076.

[23] Pham T A, Sutman M, Nadimi S. Capillary-based nonisothermal suction stress and nonlinear shear strength criteria for unsaturated compacted soils[J]. International Journal of Geomechanics, 2025, 25(5): 04025061.

[24] Mohsen A H, Albusoda B S. The collapsible soil, types, mechanism, and identification: a review study[J]. Journal of Engineering, 2022, 28(5): 41-60.

[25] Bakhtiyar K, Barno R. Numeric Simulation of Subsidence of Loess Soil under Wetting in a Limited Area[J]. Journal of Advanced Research in Fluid Mechanics and Thermal Sciences, 2023, 104(2): 1-18.

[26] Yangsukkasem N, Suebsuk J, Siriphan A, et al. Durability against cyclic wetting-drying

of cement-stabilized loess subgrade for railway in tropical semi-arid regions[J]. Construction and Building Materials, 2024, 455: 139123.

[27] Motameni S, Rostami F, Farzai S, et al. A comparative analysis of machine learning models for predicting loess collapse potential[J]. Geotechnical and Geological Engineering, 2024, 42(2): 881-894.

[28] Shafea L, Felde V J, Woche S K, et al. Microplastics effects on wettability, pore sizes and saturated hydraulic conductivity of a loess topsoil[J]. Geoderma, 2023, 437: 116566.

[29] Gramegna L, Abed A A, Sołowski W T, et al. An Elastoplastic Framework Accounting for Changes in Matric and Osmotic Suction in Unsaturated Non-expansive Clays[C]// National Conference of the Researchers of Geotechnical Engineering. Cham: Springer Nature Switzerland, 2023: 311-318.